Available online at www.sciencedirect.com
ScienceDirect
Polymer 47 (2006) 8527–8535
polymer
www.elsevier.com/locate/polymer

Properties and morphology of nanocomposites based on styrenic polymers, Part II: Effects of maleic anhydride units

H.A. Stretz [a,*], D.R. Paul [b]

[a] Department of Chemical Engineering, Tennessee Technological University, TN 38501, United States
[b] Department of Chemical Engineering and Texas Materials Institute, University of Texas at Austin, Austin, TX 78712, United States

Received 19 August 2006; received in revised form 12 October 2006; accepted 13 October 2006
Available online 3 November 2006

Abstract

Based on enhancement in exfoliation for polyolefin-*g*-maleic anhydride composites with the addition of as little as 1 wt% maleic anhydride (MA), the effect of MA in styrene–maleic anhydride copolymer (SMA)-based nanocomposites was studied. SMA nanocomposites were mixed using a DSM melt compounder followed by injection molding in a pneumatic bench top molder. These materials produced the same modulus enhancement and TEM-based areal particle densities on a weight percent basis as SAN-based nanocomposites from a previous study, but the areal TEM-based particle densities remained lower overall than literature values for polyolefin-*g*-MA mixtures. This behavior is explained by repulsive interactions between styrene and the alkyl tail of the surfactant, suggesting that polar surfactant tails could lead to improved exfoliation in styrene copolymer-based/montmorillonite nanocomposites. The role of increased melt viscosity and shearing on particle dispersion as MA is added to the copolymer is discussed.

Keywords: Maleic anhydride; Montmorillonite; Nanocomposites

1. Introduction

For many polymers addition of a nano-phase reinforcing agent such as montmorillonite clay (MMT) could add value to the balance of properties, including increased modulus, heat deflection temperature, and in some cases increased strength and reduced flammability. To realize these potential benefits, it is necessary to be able to exfoliate and disperse the high aspect ratio clay platelets more or less individually within the polymer matrix. For nanocomposites made by melt processing, there must be a good interaction between the polymer and the organoclay in order to achieve exfoliation, and this may or may not exist depending on the structure of the polymer. Good exfoliation is readily achieved in the case of polyamides, but not for polyolefins or styrenic polymers. Evidently the latter lack the polar characteristics needed to interact well with the clay surface unlike the polyamides [1]. Interestingly, it has been found that grafting as little as 1% by weight of maleic anhydride to a polyolefin dramatically improves the ability to exfoliate or disperse organoclay platelets; indeed, several commercial products employ just a few percent of a maleated polyolefin as a ‘‘compatibilizer’’ in the formulation to aid clay dispersion in the unmaleated polyolefins. As one example, Hotta and Paul have shown for linear low density polyethylene, the areal density of montmorillonite particles in transmission electron microscopic (TEM) images, increases 50-fold as maleic anhydride content is increased from 0 to 1% in the matrix [2]. A similar high specific density of MMT particles was shown in TEM images reported by Nam et al. [3] for an extruded PP-*g*-MA with only 0.2% MA in the matrix. (An excellent review of the preparation and processing of such nanocomposites, including polyolefin-based nanocomposites, is given by Ray and Okamoto [4].) The interactions that such small amounts of maleation evidently bring to such

* Corresponding author. Tel.: +1 931 372 3495; fax: +1 931 372 6352.
E-mail address: hstretz@tntech.edu (H.A. Stretz).

0032-3861/$ - see front matter © 2006 Elsevier Ltd. All rights reserved.
doi:10.1016/j.polymer.2006.10.013

formulations are not well understood. Maleic anhydride can be copolymerized with polystyrene, and other monomers like acrylonitrile, and it would be important to know if maleic anhydride incorporation into styrenic polymers facilitates exfoliation in analogy to the case of polyolefins. Compatibilization of montmorillonite in styrenic copolymer nanocomposites using maleic anhydride was previously noted by several authors [5–7] who primarily focused on synthesis but gave limited details about mechanical properties. Zheng et al. have recently reported on the use of maleic anhydride as a surfactant for compatibilization of MMT with polystyrene [8], and Ray et al. showed that surface tension was reduced for PS blends with maleated polypropylene when organoclay particles were introduced [9].

In terms of applications, polystyrene is a brittle polymer, and adding a filler to this matrix can be expected to make it more so. However, addition of high aspect ratio particles can improve barrier properties, flammability, etc. Mixtures of styrene–acrylonitrile copolymers with organoclays are important in that they serve as models for exfoliation of montmorillonite in the more complex rubber-filled systems such as ABS [10]; ABS-based nanocomposites particularly have potential application as a nonhalogenated fire retardant in computer housings [11].

This paper explores the use of various styrenic polymers that contain maleic anhydride in varying amounts to form nanocomposites from an organoclay using melt processing. Dispersion of the organoclay was evaluated by transmission electron microscopy combined with digital image analysis and by analysis of the Young's modulus of these composites. Wide angle X-ray scattering (WAXS) results are also presented.

2. Experimental

2.1. Materials

Various styrene–maleic anhydride copolymers (SMA) and two compositions of a styrene–acrylonitrile–maleic anhydride terpolymer were used; the characteristics of these polymers are given in Table 1. A single organoclay, supplied by Southern Clay Products, was used in these studies. In a previous study the structure of the surfactant modifying the montmorillonite was varied; it was found that an organoclay based on trimethyl octadecyl quaternary ammonium surfactant, led to optimum properties of nanocomposites formed from a styrene–acrylonitrile copolymer matrix with 25 wt% acrylonitrile [12]. This organoclay was formed *via* ion exchange of sodium montmorillonite with this surfactant by the supplier at 95 MER (milliequivalents per 100 g clay), an approximately stoichiometric exchange given a 92 meq/100 g cation exchange capacity for the native clay. The mass loss on ignition, 30%, is representative of the amount of organic surfactant contained in the organoclay; this experimentally determined value also includes a small contribution from the rearrangement of the silicate structure when exposed to very high temperatures [13].

2.2. Methods

All materials were dried overnight under vacuum at 80 °C prior to use. Powdered polymer and powdered organoclay were weighed and hand-mixed to form a homogenous masterbatch, and 3.2 g portions of this masterbatch were then fed into a microcompounder.

Polymer and organoclay were melt blended using a DSM intermeshing co-rotating twin screw batch microcompounder with a 5 cm^3 capacity. The screw diameter of this device tapers from 1 cm to 0.43 cm along its 10.75 cm length. Use of this microcompounder provides a basis for comparison between the SMA-based nanocomposites in the current study and SAN-based nanocomposites examined previously [14] and allows formation of injection molded parts from certain copolymers which were available only in limited quantities. Mixing was performed at 100 rpm and a barrel temperature of 220 °C for 10 min at a 1.5 mm gap between the extrusion chamber and rest stop. The normal force of the screws is reported, which correlates to the torque information commonly obtained from Brabender-type compounders.

Table 1
Description of matrix materials

Material	Supplier	Trade name	Maleic anhydride (wt%)	M_w/M_n (kg/mol)	T_g (°C)	Plateau force[a] (N)	Young's modulus (GPa)	Density (g/cm^3)	Comments
PS	Dow	Styron 678 CW	0			689	2.96	1.04	
SMA-2	Arco	Experimental	2			1063	3.00		
SMA-6	Arco	Dylark 132	6			1193	3.04		
SMA-8	Arco	Dylark 232	8	240/120	117	1306	3.06	1.08	
SMA-14	Arco	Dylark 332	14	170/90	128	1612	3.19	1.11	
SMA-25	Monsanto		25		154	2814	–		
SAN-25-MA	Bayer	Experimental	1			1763	3.30	1.07	Contains 25% AN
SAN-31-MA	Bayer	Experimental	1.3	119/57		1722	3.42	1.08	Contains 31% AN
SAN-2	Asahi	Experimental	0	204	108	956	3.03	1.04	Contains 2% AN
SAN-13.5	Asahi	Experimental	0	149		1133	3.17	1.06	Contains 13.5% AN
SAN-25	Dow	Tyril 100	0	152	107	1465	3.24	1.07	Contains 25% AN
SAN-31	Dow	Tyril 125	0	98		1580	3.27	1.08	Contains 31% AN

[a] Values measured at 220 °C, 100 rpm, 1.5 mm gap and 10 min.

Material was injection molded using a bench top pneumatic ram injection molder at an injection temperature of 215 °C and an injection pressure of 60 psi. Specimens were cooled in the mold at 80 °C for 5 min prior to removal. The molded test specimens were rectangular-shaped, measuring 0.155 × 0.4 × 3.1 cm.

Tensile modulus tests were performed on an Instron model 1137 at a crosshead rate of 0.51 cm/min using an extensometer having a 2.54 cm gage length. Three specimens for each composition were tested, showing a maximum standard deviation of 4% of the mean modulus.

The amount of pristine montmorillonite in the composite (%MMT) was calculated from an experimentally determined ash percentage (%MMT_{ash}); pre-dried microcompounder extrudate was heated at 900 °C for over 45 min.

$$\%\mathrm{MMT} = \frac{\%\mathrm{MMT_{ash}}}{0.935} \quad (1)$$

The "0.935" factor in this calculation corrects for structural rearrangement of the pristine montmorillonite during the analysis; oxidative heating of the clay has been shown to result in a 6.5% mass loss [13]. The actual percentage of organoclay, if needed, can be determined using an LoI, or "loss on ignition" value of 0.30 for this organoclay, as previously discussed [12,14].

$$\mathrm{organoclay}(\%) = \frac{\%\mathrm{MMT_{ash}}}{(1-\mathrm{LoI})} \quad (2)$$

WAXS scans were obtained using a Scintag XDS 2000 diffractometer. Injection molded samples were scanned such that the beam probed the skin of the tensile bar perpendicular to the direction of flow.

Sections for microscopy, 50 nm in thickness, were prepared using a Reichert-Jung Ultracut E cryogenic ultramicrotome with the diamond knife at room temperature. Knife speeds were 0.3–0.5 mm/s. Images were produced on a JEOL 2010 F electron microscope operating at 120 kV, and all were viewed along the axis of the flow direction.

Image analysis was performed on digitally captured images, using 350–400 particles from 8 to 30 photomicrographs. Gatan DigitalMicrograph analysis software was employed to measure the length, thickness and angle of orientation for each particle.

3. Effect of terpolymer SANMA on nanocomposite modulus

The original conception for this work was to use small amounts of maleic anhydride as an effective "compatibilizer" for organoclay dispersion in SAN or ABS formulations; a strategy proven to be very effective in polyolefin systems [3,4,15,16]. To implement such a strategy the polymer containing the maleic anhydride should be miscible with the SAN matrix of the ABS material. Terpolymers of styrene/acrylonitrile/maleic anhydride have been designed as reactive compatibilizers for ABS/polyamide systems, and the material designated as SAN-31-MA in Table 1 is one such material [17–20]. It is fully miscible with SAN polymers containing about 27–35 wt% acrylonitrile and would, in principle, be added to ABS materials based on such matrices as a "compatibilizer" for organoclay dispersion. A similar terpolymer, SAN-25-MA, was synthesized, courtesy of Dr. Allen Padwa at Bayer, specifically for this study, and would be miscible with an SAN material with 25 wt% acrylonitrile. These materials were initially compounded as a "masterbatch" with the organoclay. The concept that a compatibilized masterbatch could be produced with significant improvements in clay exfoliation did not prove to be useful as the data in Fig. 1 make clear. The Young's modulus is shown as a function of MMT content in SAN-25 and SAN-31 matrices, both with the maleic anhydride in the terpolymer and without. Addition of the organoclay to the pure SANMA material did not lead to a statistically meaningful improvement in modulus beyond that of SAN materials containing no maleic anhydride. Adding SANMA in varying amounts to SAN (not shown) likewise did not show any enhanced reinforcement or other evidence, TEM or X-ray, of improved organoclay dispersion.

One might argue that 1% MA in an SAN-based material is, unlike the case for polyolefins, not enough to provide a beneficial "compatibilizing" effect. There is another strategy for incorporating more maleic anhydride into an SAN matrix; it is well known that SAN and SMA copolymers are miscible when the contents of AN and MA are not too different [21,22]. Specifically, SAN-25 and SMA-25 are miscible and are commercially available products [23]. The miscible blend of SAN-25 and SMA-25 was prepared using a twin screw extruder employing identical conditions for processing SAN-25 nanocomposites as reported previously [12]. Nanocomposites based on this matrix were then formed on the microcompounder. The Young's modulus *versus* MMT content for such a blend is shown in Fig. 2, and compared to the case with no maleic anhydride, an SAN-25-based nanocomposite. The presence of maleic anhydride in the blend did not produce a change in

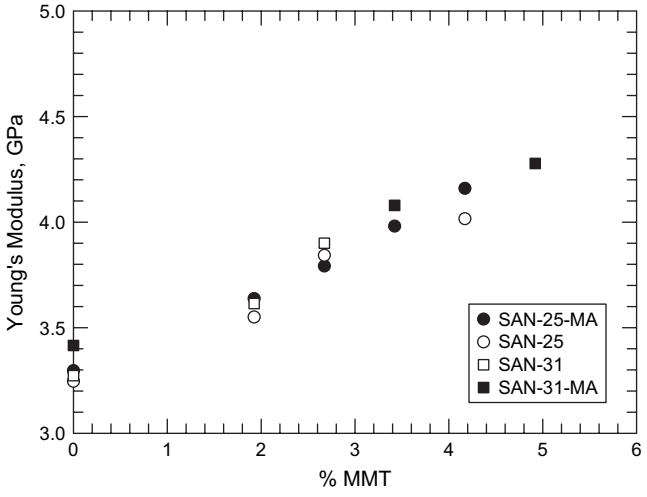

Fig. 1. Young's modulus for composites of SANMA/MMT formed with 1 wt% maleic anhydride in the terpolymer *versus* composites formed from the SAN copolymer with no maleic anhydride. In the case where the AN content is either 25 or 31 wt%, no synergistic effect was found by the addition of maleic anhydride.

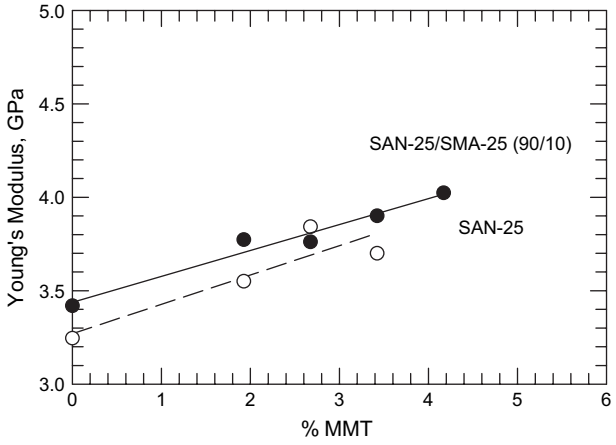

Fig. 2. Young's modulus for composites formed from a matrix of SAN-25 blended with SMA-25 in 90/10 ratio, and subsequently compounded with MMT. (Final blend of MA content is 2.5 wt%.) The corresponding moduli of the SAN-25-based nanocomposites are shown for comparison. The enhancement of modulus, or slope, is seemingly unaffected by the presence of small amounts of maleic anhydride for this system.

modulus enhancement beyond the enhancement seen for SAN-25-based nanocomposites, in contrast to the significant dispersion and modulus enhancement affected by maleic anhydride in polyolefins.

4. Nanocomposites based on styrene–maleic anhydride copolymers

If 1–3% maleic anhydride does not cause a significant enhancement for styrene–acrylonitrile-based nanocomposites, we can instead explore if varying maleic anhydride content over a wider range will produce an enhancement by using SMA-based copolymers to form nanocomposites and compare these mixtures to composites formed from PS. In this section, the morphology and mechanical properties of nanocomposites based on a series of SMA copolymers of varying maleic anhydride content, from 0 to 58 wt% MA, are described and analyzed. In the following section, we compare the SMA-based nanocomposites to nanocomposites obtained from poly(styrene-*co*-acrylonitrile) (SAN), where the styrene monomer content(s) in the two matrices are comparable.

Fig. 3 shows TEM images of a PS-based nanocomposite, with no maleic anhydride, and clearly the dispersion is poor. The particles are often micron-sized, with a few smaller platelets and stacks of platelets present in the matrix. In Fig. 4a and b, where the maleic anhydride content of the SMA is now 14 wt%, the dispersion is improved compared to the PS-based composite; montmorillonite particles are now primarily composed of smaller stacks. (Note that for Figs. 4 and 5, parts c and d represent the SAN-based mixtures to be discussed in the next section.) Fig. 5a and b shows TEM images of nanocomposites based on an SMA containing 25 wt% maleic anhydride. The particle density in the SMA-25-based material appears to be greater than for the SMA-14-based material.

Results of digital image analysis performed using images at 10K magnification are summarized in Table 2; details of how the average particle characteristics were calculated are given in a previous publication [14]. Relative to the PS-based materials, much smaller particle thicknesses are observed for maleic anhydride containing copolymers, indicating that the maleic anhydride in the copolymer does improve montmorillonite particle dispersion. The specific particle densities, which have been normalized for the amount of clay added to the mixture, show a 6–7-fold increase with 25 wt% maleic anhydride in the copolymer, compared to the 50-fold increase noted by Hotta and Paul for PE-*g*-MA nanocomposites with only 1% MA [2]. The WAXS data shown in Fig. 6a indicate that increases in maleic anhydride content do not improve intercalation, since the d_{001} peak does not shift as maleic anhydride content is increased.

The tensile moduli of the SMA-based materials are summarized in Fig. 7. These nanocomposites show a trend of increasing reinforcement as maleic anhydride content in the copolymer is increased. Note that the SMA-25 nanocomposite is not included in this analysis. During processing, the SMA-25 showed signs of degradation such as an odor of amines, despite the nitrogen purge at the feed inlet of the DSM compounder. The SMA-25-based nanocomposite foamed on opening the purge valve to the atmosphere. This material was also quite difficult

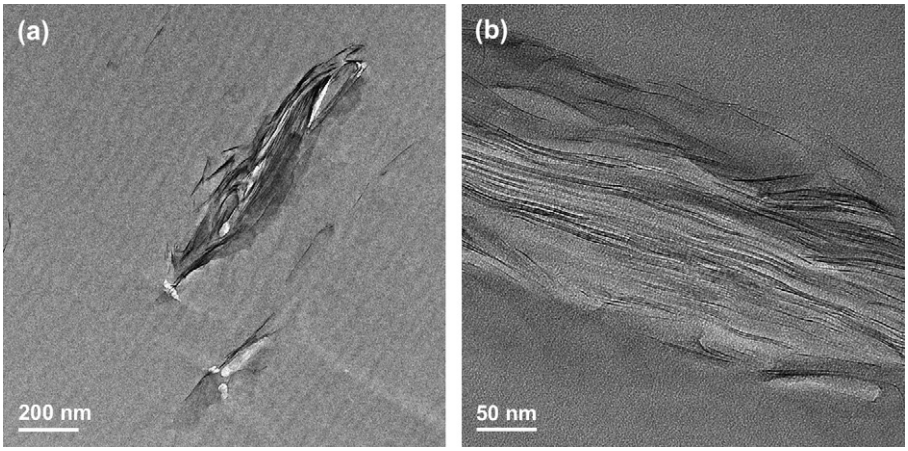

Fig. 3. TEM photomicrographs of the PS/$M_3(C_{18})$composite, 3.2% MMT, viewed along the flow direction.

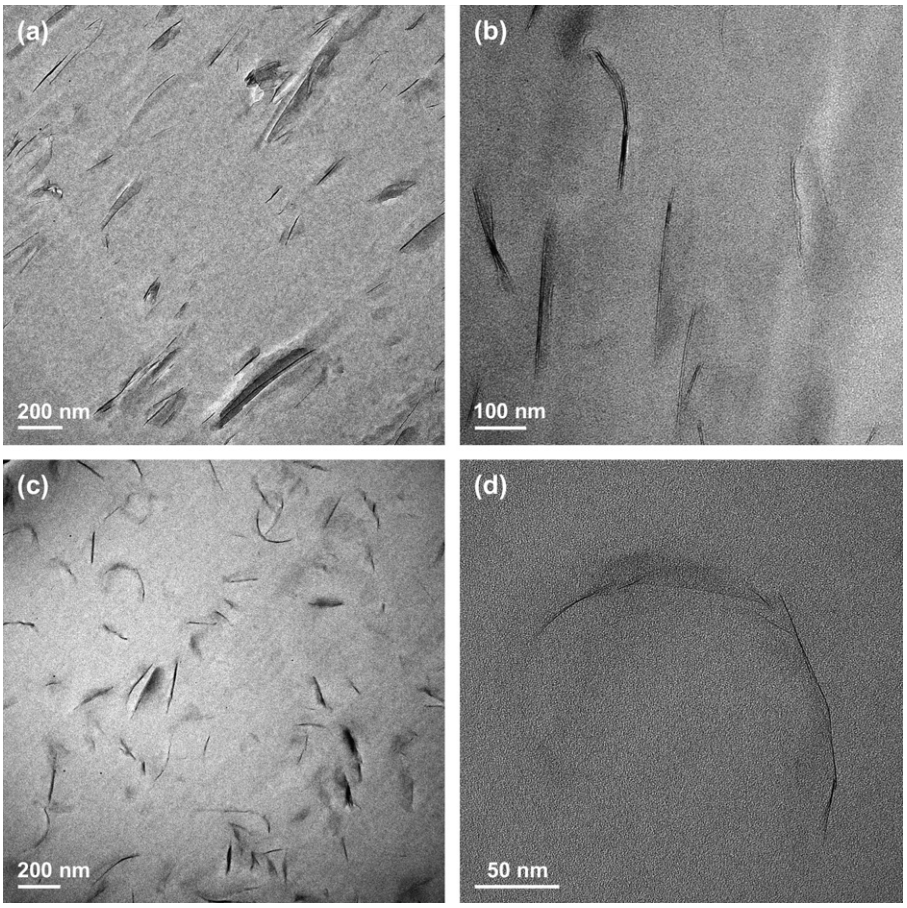

Fig. 4. TEM photomicrographs of the (a and b) SMA-14/$M_3(C_{18})$ composite *versus* the (c and d) SAN-13.5/$M_3(C_{18})$ composite, 3.2% MMT, viewed along the flow direction.

to mold; although it could be transferred to the mold chamber, the final molded part exhibited bubbles. Consequently TEM analysis was possible for the final SMA-25-based molded part, but WAXS or modulus analysis was not.

5. Comparison of nanocomposites based on styrene–maleic anhydride copolymer *versus* styrene–acrylonitrile copolymer

In order to benchmark these results, we can compare the results for SMA-based nanocomposites with previous studies of nanocomposites based on styrene–acrylonitrile copolymer (SAN), where the levels of styrene in the copolymer (weight %) are comparable.

Fig. 4c and d shows TEM images of nanocomposites based on an SAN containing 13.5 wt% acrylonitrile which are quite similar to the previously discussed SMA-14-based nanocomposites shown in Fig. 4a and b. Also, Fig. 5c and d shows an SAN-25-based nanocomposite, and again the images show very similar particle sizes and particle density to that seen for SMA-25-based nanocomposites from Fig. 5a and b. Qualitatively these co-monomers led to similar increases in filler dispersion, *i.e.*, for a given weight % of acrylonitrile gives about the same result as a similar amount of maleic anhydride. Digital image analysis results shown in Table 2, confirm that the average particle length, thickness, aspect ratio and particle density for the SMA-based materials are very similar for a given MA or AN content.

However, the d_{001} peak shift of SMA-based composites given in Fig. 6a is greater than that for the SAN-based nanocomposite results given in Fig. 6b. As discussed previously for SAN-25-based nanocomposites, no consistent correlation has been noted between improved intercalation and improved dispersion in these composites [12]. In this case, comparison of WAXS results to TEM images indicates the same conclusion, *i.e.*, the greater shift in the d_{001}-spacing ($\Delta d_{001} = d_{001,\ \text{composite}} - d_{001,\ \text{organoclay}}$) for the SMA-based materials did not produce, for instance, significantly greater particle density for SMA-based *versus* SAN-based materials.

In order to compare the reinforcement effect of the organoclay in the different copolymers, a uniform or normalized basis must be adopted which accounts both for the increased modulus of the matrix as maleic anhydride content is increased, and for the decreasing potential of the matrix to be reinforced. The reinforcement effect can be defined as a slope of the plot of normalized modulus *versus* filler content. The reinforcement factor, RF_w, is simply the limit of this slope as the filler content approaches zero, uniquely defining a single slope for a single plot.

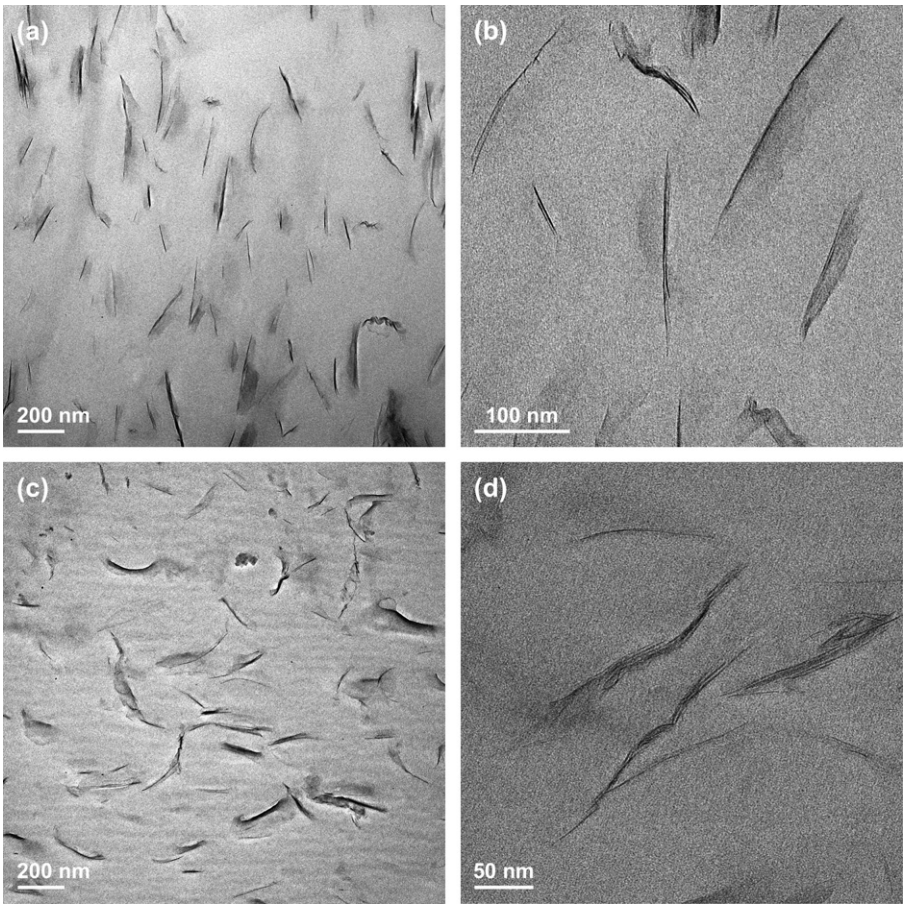

Fig. 5. TEM photomicrographs of the (a and b) SMA-25/$M_3(C_{18})$ composite *versus* the (c and d) SAN-25/$M_3(C_{18})$ composite, 3.2% MMT, viewed along the flow direction.

$$RF_w = \lim_{w_{platelets} \to 0} \frac{d[E/E_m]}{dw_{platelets}} \quad (3)$$

Eq. (3) is based on weight fraction of the filler ($w_{platelets}$), defined as such for practical reasons, but is easily converted to a reinforcement factor based on volume-fraction (RF), a parameter used in model predictions [10].

The RF_w values for the SMA-based nanocomposites are shown as the solid circles in Fig. 8. These data clearly indicate improved reinforcement as the maleic anhydride content of the matrix copolymer is increased. A comparison to the SAN-based nanocomposites (indicated by a solid line in Fig. 8, original data published by Stretz and Paul [14]), however, indicates that on a weight percent basis, the effect of adding maleic anhydride is only slightly greater than the effect of adding

Table 2
Image analysis of TEM photomicrographs[a]

Copolymer	Number avg. length (nm) $\overline{l_n}$	Number avg. thickness (nm) $\overline{t_n}$	Estimated number of platelets per stack	Aspect ratio $\overline{l_n}/\overline{t_n}$	Number avg. aspect ratio $\langle l/t \rangle_n$	TEM particle density[b] (μm^{-2})	Specific particle density[c] (μm^{-2})
SMA-based nanocomposites							
PS	276	14.9	6.1	18.5	41.3	3.88	1.2
SMA-6	137	8.8	3.2	15.6	25.6	13.3	4.2
SMA-14	129	4.6	2.2	27.9	36.3	18.4	5.8
SMA-25	144	6.6	2.7	21.7	34.5	23.6	7.4
SAN-based nanocomposites							
PS	276	14.9	6.1	18.5	41.3	3.9	1.2
SAN-13.5	126	6.1	3.3	20.6	27.1	20.0	6.3
SAN-25	148	5.6	3.1	26.5	38.3	16.5	5.2

[a] All data are taken from images viewed along the flow direction.
[b] The TEM particle density is the average number of montmorillonite particles per μm^2.
[c] The specific particle density is the (TEM particle density)/(MMT concentration), where MMT = 3.2 wt%.

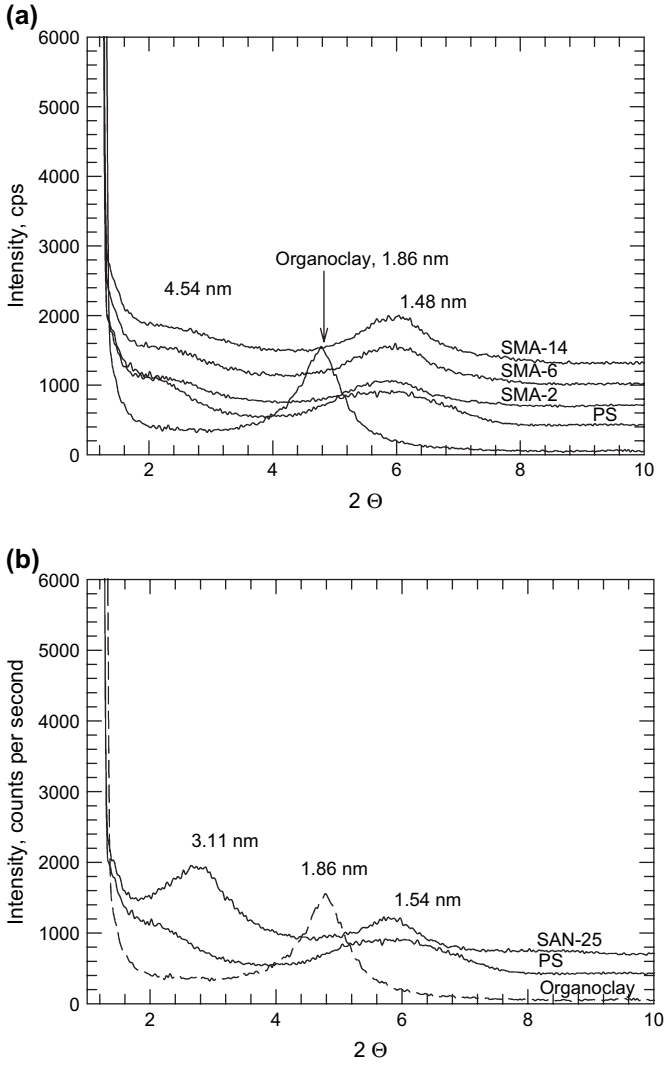

Fig. 6. WAXS scans for (a) SMA/$M_3(C_{18})_1$ composites where weight % MA in the copolymer is indicated. All composites contain 3.2% MMT. The lowest WAXS scan is for the pristine organoclay, and all other scans are shown with baselines incremented by 300 cps for clarity. For comparison, the analogous WAXS scans for (b) SAN/$M_3(C_{18})_1$ composites are given.

acrylonitrile to the copolymer matrix. Qualitatively, this conclusion is consistent with the TEM images shown earlier.

6. Effect of shear stress on exfoliation efficiency

In a complex environment such as in melt processing, particle dispersion would be expected to be affected by many factors in addition to the inherent driving force arising from interactions between copolymer and organoclay. Among these additional factors is the shear stress experienced by the particle during mixing. Shear stress is a function of melt viscosity, which can vary with the identity of the matrix. Therefore, it is useful to consider how shear stress varied as the polymer matrix was changed. Fig. 9 shows that as maleic anhydride content is increased in the copolymer, the axial force produced by the screws (at constant 100 rpm) increases substantially. In comparison, an equivalent weight percent of acrylonitrile

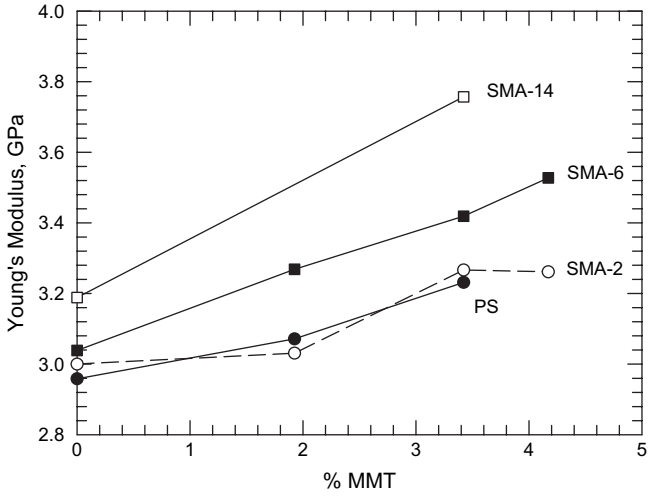

Fig. 7. Young's modulus for composites of SMA/MMT formed from various maleic anhydride contents (weight %) of the SMA copolymer.

produces a lower force than when maleic anhydride is in the copolymer. Thus, we compare the effect of the force for the SMA-based and SAN-based nanocomposites on the final modulus enhancement as measured by exfoliation efficiency in Fig. 10. For a given force, or shear stress on the particle, the SMA copolymers produce a reinforcement factor comparable to that of the SAN copolymers. Therefore, if shear stress on the particle also contributes to montmorillonite particle dispersion, then it may be that the maleic anhydride units promote interactions similar to that of acrylonitrile units as measured by their effect on exfoliation and reinforcement.

7. Discussion

The interaction of an organoclay with the polymer matrix is believed to be a key factor determining whether a

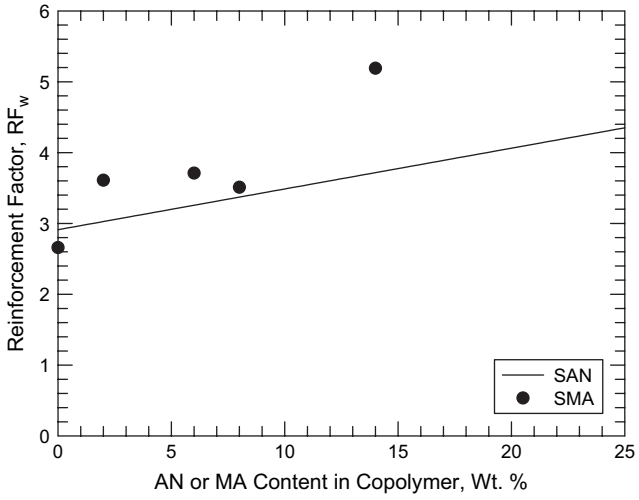

Fig. 8. Reinforcement factors, RF_w, for composites of SMA/MMT formed from various maleic anhydride contents (weight percent) of the SMA copolymer *versus* the analogous effect for acrylonitrile weight percent in composites formed from SAN copolymers. SAN data are indicated by a solid line; original data points available in Stretz and Paul [14].

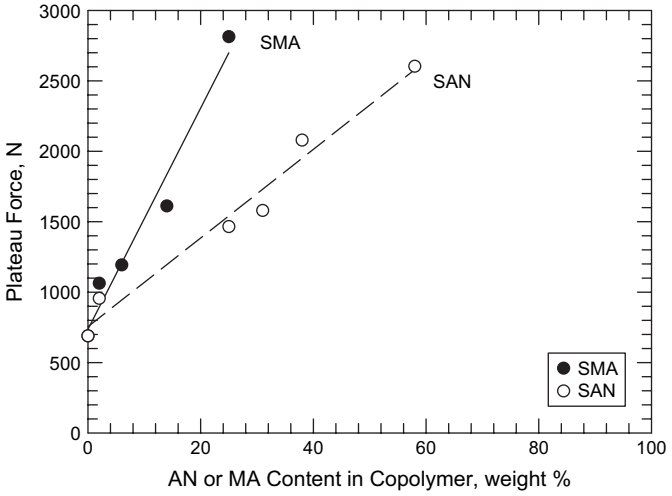

Fig. 9. Variation of the plateau force, a reflection of increasing melt viscosity, for the various maleic anhydride contents (weight percent) in the SMA copolymer. The analogous plateau force experienced during compounding for SAN-based copolymers is also shown.

well-exfoliated nanocomposite is formed or not during melt processing. Polyamides seem to interact well with a well-selected organoclay, and as a result, these matrices, especially nylon-6, seem to lead to the best exfoliated nanocomposites reported to date [24]. On the other hand, polyolefins and styrenic polymers do not appear to interact favorably with organoclays, and generally these materials do not lead to nanocomposites exhibiting very high levels of reinforcement or other property enhancements. Interestingly, addition of less than ~1% maleic anhydride into polyolefin systems by grafting onto the polyolefin backbone, or even using this maleated component as a "compatibilizer" added in small amounts to the base polyolefin, produces great improvement in the dispersion of the organoclay and leads to significant property improvements. In the case of styrenic copolymers, addition of maleic anhydride leads to much less dramatic enhancement. Particle dispersion and modulus enhancement are not improved

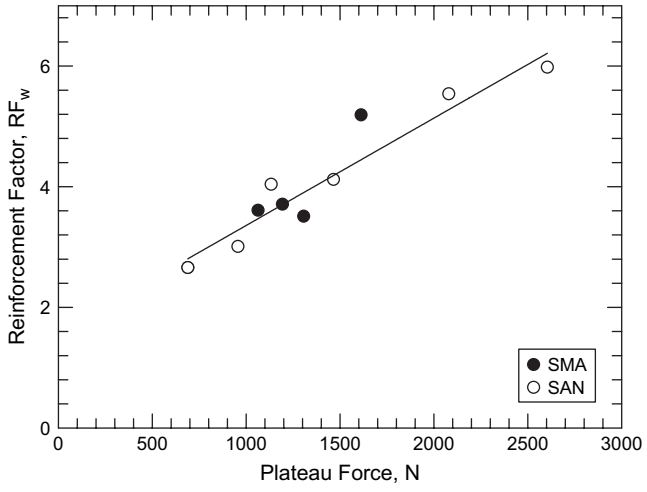

Fig. 10. Reinforcement factors, RF_w, for SMA-based nanocomposites *versus* plateau force. SAN-based nanocomposites are also given for comparison.

substantially when compared to addition of other monomers such as acrylonitrile. Furthermore, the specific particle densities from TEM image analysis shown in Table 2 are approximately 8 particles/μm^2 for the SMA-based nanocomposites, far below the 100–120 particles/μm^2 reported for well-exfoliated nanocomposites formed from nylon-6 by Chavarria and Paul [25], the ~50 particles/μm^2 which can be counted in TEM images of PE-*g*-MA nanocomposites reported by Hotta and Paul [2], or the ~50 particles/μm^2 which can be counted in TEM images of PP-*g*-MA nanocomposites reported by Nam et al. [3].

The question is why does maleic anhydride fail to provide the same magnitude of benefit for nanocomposites based on styrenic polymers as observed in polyolefins? We offer the following explanation based on our evolving understanding of the organoclay–polymer interaction which we believe is the key, but not only, factor responsible for achieving high levels of dispersion and, thus, performance in nanocomposites.

There are numerous thermodynamic interactions at play in determining how well clay platelets can be dispersed in a given polymer. It is first necessary to reduce to some degree the platelet–platelet cohesive force which is effectively done by adding the organic surfactant; since similar surfactants are employed in the cases of interest here, this interaction is effectively fixed in this study. Interactions of the polymer with the silicate surface and with the surfactant may, however, be altered as the surfactant structure is changed. Surfactant structure can affect the access of the polymer to the silicate surface, but not the intrinsic affinity, or lack thereof, of the polymer for the silicate surface [26]. We believe that polyamides exfoliate certain organoclays very efficiently because of their strong affinity for the silicate surface and, in spite of, the obviously repulsive interaction of mixing polyamide with the hydrocarbon tails of the surfactant [27]. Polyolefins would be expected to have very poor affinity for the silicate surface [2,28]; however, their interaction with the hydrocarbon tails of the surfactant would be only weakly repulsive (polypropylene) or even neutral (polyethylene). Incorporating polar anhydride groups would seem to increase the affinity for the silicate surface which apparently is enough to greatly improve the polymer–organoclay dispersion since the bulk of the polymer matrix interacts neutrally or weakly with the hydrocarbon tails of the surfactant. It could be argued that styrenic segments might interact somewhat less repulsively with the silicate surface than does the saturated structure of a polyolefin; however, it is clear that the interaction of styrenic segments with the hydrocarbon tails of the surfactant is very repulsive. Note that polyethylene and polystyrene are grossly incompatible compared to any mixture of polyolefins [29–31].

Ziaee and Paul [32] have determined the Van Laar binary interaction energy density between styrenic and ethylenic units to be 7–8 cal/cm^3. The latter would be near zero for the interaction among olefinic repeat units. Even though maleic anhydride units, and possibly acrylonitrile units, may improve the interaction of the polymer with the silicate surfactant, this does not seem to be able to overcome the repulsive interaction of the polymer with the surfactant which becomes more

repulsive as MA or AN is added. Thus, it appears that it is the very different polymer–surfactant interactions that allow small amounts of maleic anhydride to be so effective for polyolefins but not for styrenic polymers. We, therefore, suggest that the repulsive interactions between the styrene and the alkyl-based tail of the surfactant are substantial and future work should examine whether altering this chemistry will allow the maleic anhydride to perform better as a compatibilizer in styrenic copolymer-based nanocomposites with montmorillonite organoclays.

8. Conclusion

Grafting as little as 1% by weight of maleic anhydride (MA) to a polyolefin dramatically improves the ability of the polymer to disperse organoclay platelets during melt processing. In contrast, the results of this study indicate that adding 1% MA into a poly(styrene–acrylonitrile) terpolymer (SANMA) does not produce a corresponding increase in dispersion or modulus enhancement when compared to SAN-based nanocomposites. Given that 1% maleic anhydride in SAN might not be enough to provide a beneficial ''compatibilizing'' effect, nanocomposites based on poly(styrene–maleic anhydride) (SMA) with as much as 25 wt% maleic anhydride in the copolymer were used to form nanocomposites with a trimethyl octadecyl ammonium-modified organoclay. The modulus values from these composites were normalized for the effect of the matrix modulus. The SMA-based nanocomposites showed significant improvement in both TEM measurements of particle dispersion and in modulus enhancement when compared to the PS-based nanocomposite. Digital image analysis of TEM photomicrographs, for instance, showed a 6–7-fold increase in particle densities compared to the PS-based composites. Styrenic copolymers with comparable weight percents of acrylonitrile *versus* maleic anhydride produced comparable increases in composite reinforcement as well as similar particle densities in the TEM images. While slightly higher levels of reinforcement were noted in the SMA-based nanocomposites, this improvement correlated with the higher melt viscosity (measured as an axial force from rotation of the screws) of the SMA copolymers as compared to SAN copolymers, resulting in greater shear stress on the particles during mixing.

The difference between the effectiveness of maleic anhydride as a compatibilizer for grafted polyolefins where only ~1 wt% is necessary, compared to copolymers of polystyrene where 25 wt% produces measurable improvements, is suggested to be due to the balance of interactions between the organoclay components and the matrix polymer. Apparently introduction of maleic anhydride into the copolymer is insufficient to overcome repulsions between the polymer and the alkyl-based tails of the surfactants, particularly at low copolymer MA content. Future work should examine whether altering the surfactant tail chemistry allows the maleic anhydride to perform better as a compatibilizer in styrenic copolymer-based nanocomposites with montmorillonite organoclays.

Acknowledgements

The authors would like to thank the Air Force Office of Sponsored Research for funding. We gratefully acknowledge interactions with the staff of Southern Clay Products, who provided materials and advice, including the WAXS performed by Tony Gonzales. Dr. JP Zhou at the Center for Nano and Molecular Science and the Texas Materials Institute, University of Texas at Austin provided electron microscopy support. Thanks to Allen Padwa at Bayer for the terpolymers, specifically for providing the SAN-25-MA synthesis, and for generous advice. Thanks to our other suppliers including Dow Chemical, Asahi and Monsanto for the SAN and SMA copolymers.

References

[1] Fornes TD, Yoon PJ, Paul DR, Hunter DL, Keskkula H. Polymer 2002; 43:5915.
[2] Hotta S, Paul DR. Polymer 2004;45:7639.
[3] Nam PH, Maiti P, Okamoto M, Kotaka T, Hasegawa N, Usuki A. Polymer 2001;42:9633.
[4] Ray SS, Okamoto M. Prog Polym Sci 2003;28:1539.
[5] Mitsunaga M, Ito Y, Ray SS, Okamoto H, Hironaka K. Macromol Mater Eng 2003;288:543.
[6] Wang D, Wilke CA. Polym Degrad Stab 2003;80:171.
[7] Salahuddin N, Akelah A. Polym Adv Technol 2002;13(5):339.
[8] Zheng X, Jiang DD, Wilke CA. Polym Degrad Stab 2006;91:103.
[9] Ray SS, Pouliot S, Bousmina M, Utracki LA. Polymer 2004;45: 8403.
[10] Stretz HA, Paul DR. Polymer 2005;46:3818.
[11] Hu Y, Wang S, Zong R, Tang Y, Chen Z, Fan W. Appl Clay Sci 2004; 25:49.
[12] Stretz HA, Paul DR, Keskkula H, Li R, Cassidy PE. Polymer 2005;46(8): 2621.
[13] Suter UW, Osman MA, Ploetze M. J Mater Chem 2003;13:2359.
[14] Stretz HA, Paul DR. Polymer 2006, in press. doi:10.1016/j.polymer.2006.09.049.
[15] Hasegawa N, Okamoto H, Kato M, Usuki A. J Appl Polym Sci 2000;78: 1918.
[16] Kato M, Usuki A, Okada A. J Appl Polym Sci 1997;66:1781.
[17] Kudva RA, Keskkula H, Paul DR. Polymer 2000;41:239.
[18] Kitayama N, Keskkula H, Paul DR. Polymer 2000;41:8041.
[19] Kitayama N, Keskkula H, Paul DR. Polymer 2000;41:8053.
[20] Lavengood RE, Padwa AR, Harris AF. US 4,713,415, Monsanto; 1987.
[21] Molau GE. Polym Lett 1965;3:1007.
[22] Schmitt BJ. Makromol Chem 1980;181:1655.
[23] Kim JH, Barlow JW, Paul DR. J Polym Sci Part B Polym Phys 1989; 27(2):223.
[24] Fornes TD, Yoon PJ, Keskkula H, Paul DR. Polymer 2001;42:9929.
[25] Chavarria F, Paul DR. Polymer 2004;45:8501.
[26] Fornes TD, Paul DR, Hunter DL. Macromolecules 2004;37:1793.
[27] Ellis TS. Polym Eng Sci 1990;30(17):998.
[28] Shah RK, Hunter DL, Paul DR. Polymer 2005;46:2646.
[29] Cheung YW, Guest MJ. J Polym Sci Part B Polym Phys 2000;38(22): 2976.
[30] Locke CE, Paul DR. J Appl Polym Sci 1973;17:2597.
[31] Locke CE, Paul DR. J Appl Polym Sci 1973;17:2791.
[32] Ziaee S, Paul DR. J Polym Sci Part B Polym Phys 1996;34:2641.